Clay Minerals, (2017) **52**, 217–233

Clay minerals in shales of the Lower Silurian Longmaxi Formation in the Eastern Sichuan Basin, China

GENG YI-KAI[1], JIN ZHEN-KUI[1,*], ZHAO JIAN-HUA[1,2], WEN XIN[1], ZHANG ZHEN-PENG[3] AND WANG YANG[3]

[1] *College of Geosciences, China University of Petroleum(Beijing), Beijing 102249, China*
[2] *State Key Laboratory of Shale Oil and Gas Enrichment Mechanisms and Effective Development, Beijing 100083, China*
[3] *No. 2 Oil Production Plant, Daqing Oilfield Company, Daqing, Heilongjiang 163257, China*

(*Received 23 December 2016; revised 10 April 2017; Editor: George Christidis*)

ABSTRACT: The present study examines the characteristics of clay minerals in shale gas reservoirs and their influence on reservoir properties based on X-ray diffraction and scanning electron microscopy. These analyses were combined with optical microscopy observations and core and well-log data to investigate the genesis, distribution characteristics, main controlling factors and pore features of clay minerals of the Lower Silurian Longmaxi Formation in the East Sichuan area, China. The clay mineral assemblage consists of illite + mixed-layer illite-smectite (I-S) + chlorite. This assemblage includes three sources of clay minerals: detrital, authigenic and diagenetic minerals. The lower section of the Longmaxi Formation in the Jiaoshiba area has sealing ability which resulted in abnormal high pressures during hydrocarbon generation which inhibited illitization. Therefore, an anomalous transformation sequence is present in which the mixed-layer I-S content increases with depth. This anomalous transformation sequence can be used to infer the existence of abnormal high pressures. The detrital components of the formation also affect the clay-minerals content indirectly, especially the abundance of K-feldspar. The transformation of mixed-layer I-S to illite is limited due to the limited availability of K^+, which determines the extent of transformation. Three types of pores were observed in the shale reservoir rocks of the Longmaxi Formation: interparticle (interP) pores, intraparticle (intraP) pores and organic-matter pores. The clay-mineral content controls the development of intraP pores, which are dominated by pores within clay particles. For a given clay mineral content, smectite and mixed-layer I-S were more conducive to the development of shale-gas reservoirs than other clay minerals.

KEYWORDS: Abnormal high pressure, clay mineral, Shale reservoir, Longmaxi Formation, Eastern Sichuan Basin, China.

The term ‘clay mineral’ is generic and describes finely divided, hydrous layer silicates and hydrous amorphous silicate minerals (Li, J. *et al*., 2012). Clay minerals have a widespread distribution and unique physicochemical properties and mode of origin, making them important in terms of petroleum-geology applications (Sun *et al*., 1998; Zhou *et al*., 2005; Liu *et al*., 2009). The types and distribution of clay minerals vary in different regions and geological formations due to a number of factors. Analysis of clay-mineral composition, genesis and distribution may be used not only for

*E-mail: 85147477@qq.com
https://doi.org/10.1180/claymin.2017.052.2.04

palaeo-environmental reconstructions and records of diagenetic conditions, but may contribute in the prediction of oil and gas reserves (Daoudi *et al.*, 2010; Zhang *et al.*, 2013).

Research on shale gas in China has intensified gradually through increasing exploration and development of unconventional oil and gas reservoirs. This research has determined that research ideas and methods other than the traditional model of self-generation and self-storage used for conventional oil and gas reservoirs should be deployed (Wang *et al.*, 2014). Clay minerals are the main components of mud shales, and are also important as cement in sandstones. Clay minerals are closely related to natural gas in reservoirs composed mainly of mud shales or interlayer sandstones (Zhao *et al.*, 2008). Shale-gas exploration of the Upper Ordovician Wufeng Formation-Lower Silurian Longmaxi Formation in the East Sichuan area has good prospects; nevertheless the reservoir-forming conditions for the shale gas in this area are complicated (Zhang *et al.*, 2013; Zhao *et al.*, 2016). Understanding the genesis, distribution and evolution of clay minerals in the Longmaxi Formation shale in the eastern Sichuan area is of significant theoretical and practical importance, therefore, for marine shale-gas exploration in this area (Wang *et al.*, 2014).

The Sichuan Basin is located in the western part of the Yangtze Platform, with the Hunan-Guizhou-Hubei thrust belt in the east, the Emeishan-Liangshan thrust belt in the south, and the Micangshan uplift-Dabashan fold belt in the north (Zeng *et al.*, 2011) (Fig. 1). Uplift and expansion of the Yangtze Sea, especially the upper Yangtze Sea, formed a closed, low-energy anoxic, marine environment (Wang *et al.*, 1993; Ma *et al.*, 2004; Zhao *et al.*, 2016). The Upper Ordovician Wufeng Formation-Lower Silurian Longmaxi Formation shale is widespread throughout the Yangtze Block, except in the Yunnan-Guizhou Uplift, and is one of the main source rocks in the Sichuan Basin as well as one of the major shale-gas-producing layers. The shale occurring in the Lower Silurian Longxi Formation is mainly black shale and silty mudstone (shale), locally composed of siliceous mudstone (Li, J. *et al.*, 2012). Bentonites generally exist at the bottom of Longmaxi Formation (Su *et al.*, 2002; Liu *et al.*, 2013). The study area is located in the Jiaoshiba area in the eastern part of the Sichuan Basin and the surrounding areas, with the Central Sichuan Uplift to the northwest and Central Guizhou-Xuefeng Uplift to the south (Fig. 1). Caledonian movement was active during the Middle Ordovician–Silurian period, which resulted in the formation of several palaeo-uplifts. These palaeo-uplifts and early old lands were major sediment provenance areas for the shales (Zeng *et al.*, 2011). The Central Guizhou Oldland and Xuefeng Uplifts provided most of the terrigenous detrital material (Wang *et al.*, 1993; Li, Y. *et al.*, 2012), while the Central Sichuan Uplift was not a main supply area. Based on extensive X-ray diffraction (XRD) and scanning electron microscopy (SEM) analysis combined with optical microscopy (OM), core and well-log data and with some XRD data from Well E (Jin *et al.,* 2015), this study analysed the genesis, distribution characteristics and clay minerals and their main controlling factors in the Lower Silurian Longmaxi Formation.

SAMPLING AND ANALYTICAL METHODS

Four hundred and eight samples were selected for analysis from cores of four wells in the Longmaxi Formation (Wells A–D) in the Jiaoshiba area and Well E in the Pengshui area in the eastern Sichuan Basin. Samples were collected every 1–10 m, based on the distribution and development of the rocks. Analysis of the whole-rock and clay-mineral components of the samples was performed, using XRD, at the National Geological Experimental Testing Center using an X'Pert PRO MPD X-ray diffractometer (PANalytical) and at the State Key Laboratory of Petroleum Resources and Prospecting of China University of Petroleum (Beijing) using a D8 Advance X-ray diffractometer (Bruker). Quantitative analysis of the mineral components was based on Chinese Oil and Gas Industry Standard SY/T 5163-2010. The XRD analysis of the bulk sediments was performed at 22°C and 30% RH, and the equilibrated powdered samples were pressed into sample holders and analysed with Cu-$K\alpha$ radiation at 35 mA and 40 kV, using emitting and receiving slits of 4 and 0.5 mm, respectively, between 7 and 45°2θ. The clay fraction was extracted by the suspension method, as follows: 10 g of sample was added to 50 mL of distilled water and then left to stand in suspension for 6–8 h. The clay fraction was extracted by centrifugation and sedimented on glass slides. The XRD analysis of the clay fractions was performed with Cu-$K\alpha$ radiation using emitting and receiving slits of 2 and 0.3 mm width, respectively, in the range 0–30°2θ. Air-dried samples, ethylene glycol (EG)-solvated samples prepared in a dessicator for at least 7 h at 40–50°C, and samples heated at 550°C for 2 h (T samples) were prepared (Strixrude & Peacor, 2002).

Analysis by SEM was performed using an FE-SEM HITACHI S-4800 SEM and the energy-dispersive spectroscopic analysis (EDS) was performed with an

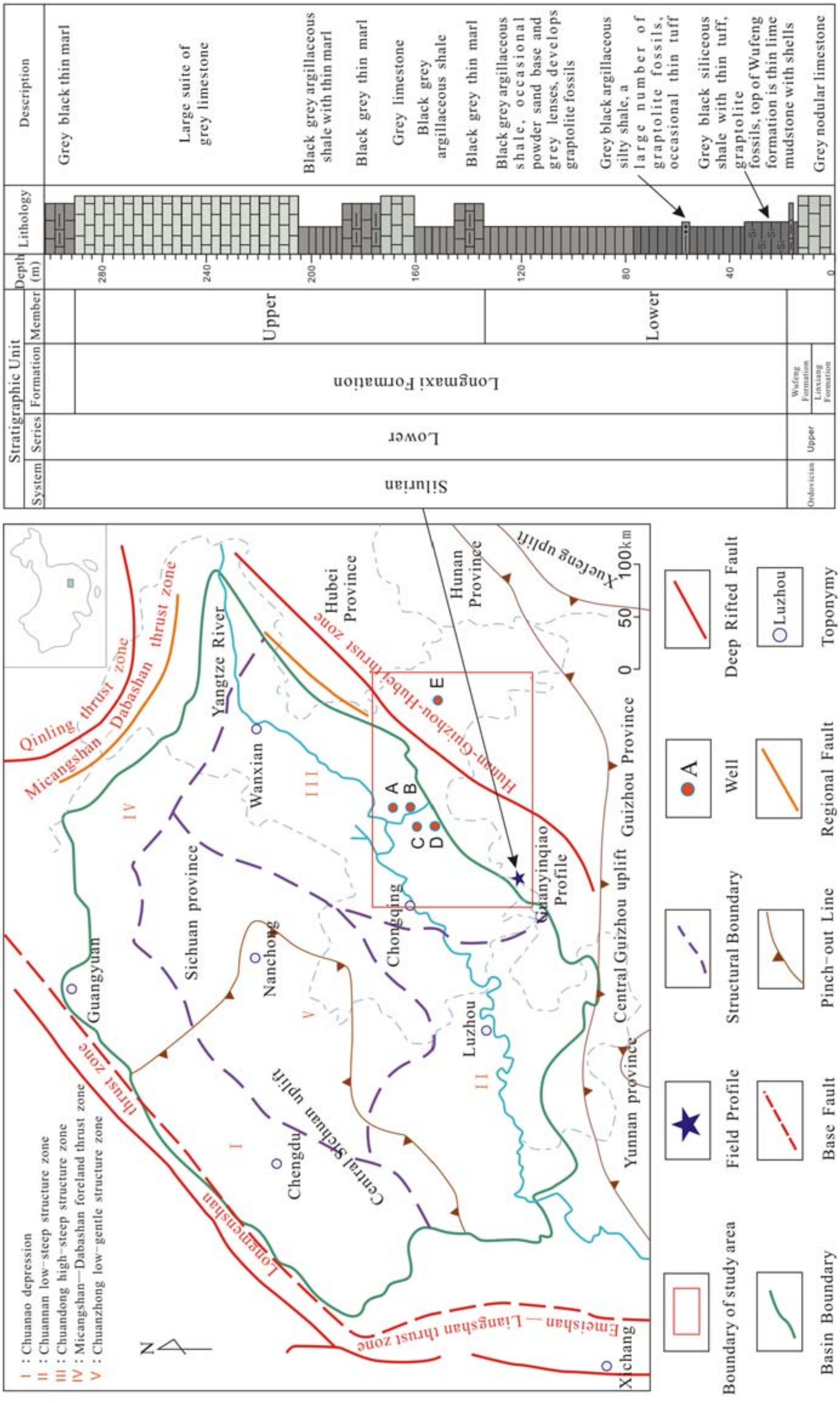

FIG. 1. Sichuan Basin structure (modified from Wang *et al.*, 2014), drilling locations and stratigraphic lithology features of the Longmaxi Formation.

EMAX-350 spectrometer at the Analytical and Testing Center of Beijing Normal University on Pt-sputtered samples (E-1045 sputter). Observation of the samples after argon ion polishing was performed using an FEI Quanta 650 SEM in the China National Center for Nanometer Petrophysics, and the State Key Laboratory of Petroleum Resources and Prospecting at China University of Petroleum (Beijing). Vitrinite reflectance (R_o) was performed using an MPV-III microphotometer in accordance with Chinese Oil and Gas Industry Standard (SY/T 5124-2012) at the State Key Laboratory of Petroleum Resource and Prospecting at China University of Petroleum-Beijing.

RESULTS

Mineralogical and geochemical characteristics

The clay mineral content determined by XRD varied between 7.5 and 73.3%, with most samples being in the range 30–50%; the quartz content ranged between 6 and 76.1% (average 39.4%); the feldspar content ranged between 2 and 29.3% (average 8.4%) with plagioclase being more abundant than K-feldspar; the carbonate content was 0–54.6% (average 8.9%,) and the pyrite content was 1.3–11.1% (average 3.8%). The clay minerals consist mainly of illite and mixed-layer I-S, and to a lesser extent of chlorite. The illite content ranged between 10 and 72% (average 40.4%), the mixed-layer I-S content ranged between 10 and 85% (average 44.9%), and the chlorite content between 1 and 55% (average 15.6%); one sample in Well D contained as much as 80% chlorite. Discrete smectite, kaolinite and mixed-layer chlorite-smectite were absent. Chlorite is derived mainly from terrigenous detrital material, and therefore the transformation sequence of clay minerals is smectite – mixed-layer I-S – illite (Zhao & He, 2008).

The quantitative mineralogical composition and the thermal maturity of the shale samples from Wells B and E are listed in Table 1. The clay-mineral content decreased and that of quartz increased from top to bottom in the Longmaxi Formation. The relative percentage of illite and chlorite increased and that of mixed-layer I-S decreased with increasing depth. The smectite content in mixed-layer I-S was 5–10%. The R_o increased with increasing depth in Well B and the maximum value was 4.14%. That R_o in Well E did not display an obvious trend but almost always exceeded 2.0% indicated a high level of maturity in the Longmaxi Formation shale.

Clay-mineral characteristics with different genetic types

The main components of mud shale, clay minerals and silt, form by weathering, transport and deposition in detrital form (Hillier, 1995; Guo *et al.*, 2004). However, the clay-mineral contents in the Paleozoic mud shales of the Sichuan Basin are generally smaller than those in terrestrial source rocks and terrigenous sediments in coastal areas, in modern lacustrine sediments and in pelagic clays, indicating that not all of these shale types were derived from terrigenous detritus (Fu *et al.*, 2011).

Characteristics of detrital clay minerals. The detrital clay minerals are generally degraded due to various degrees of weathering, transport, deposition, and other transformation processes (Fu *et al.*, 2011). Under the SEM, these clay minerals appear poorly crystalline and often occur in aggregated or dispersed form (Wu *et al.*, 1997; Liu *et al.*, 1998).

The SEM study showed that the mud shales of the Longmaxi Formation contain a large proportion of detrital clay minerals, mainly illite and chlorite. Illite exhibits bent sheet or detrital plate-like shapes, with slightly oriented but incomplete crystals (Fig. 2a–c). Transformation of feldspar and other aluminosilicate minerals may produce such illite crystal forms. Chlorites exhibit sheet-like or plate-like shapes with crystals exhibiting uneven edges and irregular shapes (Fig. 2d,e). In climatic conditions that produce intense physical weathering, parent rocks rich in illite and chlorite may be eroded, transported and re-deposited to form sediments with high concentrations of these phases (Zhang, 1992; Jin *et al.*, 2007).

Characteristics of authigenic and diagenetic clay minerals. A few authigenic illite crystals formed from altered mica were observed during SEM examination. Such illites are lath-shaped, well-stratified, and well crystallized, with crystals of uniform size. Therefore, the layered aggregates of such illites are even-sided (Fig. 2f) with K^+ contents greater than those of detrital illites (Table 2) and are often accompanied by mica platelets (Fig. 2g). Morphologically, it is difficult to distinguish authigenic illite and altered mica, which may be the result of pre-depositional weathering, or syn/post-depositional processes. They are different in terms of composition, however, especially the K^+ content. The K_2O content of authigenic illite (<9%) is generally less than that of mica (>9%, ~10%) (Table 2; Anderson & Rowley, 1981; Miller *et al.*, 1981; Zhang *et al.*, 2010; Liang *et al.*, 2012).

TABLE 1. Mineral composition and thermal maturity of shale samples from Wells B and E.

		Mineralogical composition relative percentage (%)					Clay-mineral composition relative percentage (%)				
Sample	Depth (m)	Clay	Quartz	Feldspar	Carbonate	Pyrite	Illite	Mixed-layer	Chlorite	S% in I-S	R_o (%)
B-1	2452	73.3	23.7	3	0	0	49	29	22	5	1.47
B-2	2460.27	59.4	31.6	6.3	0	2.7	41	30	29	5	
B-3	2495.35	42.2	41.7	14.3	1.8	0	44	41	15	10	2.77
B-4	2504.59	51.6	35.7	3.4	7.6	1.7	40	36	24	5	
B-5	2516	40.9	35	12.4	8.4	3.3	41	41	18	5	
B-6	2523.11	43.9	38.6	7.1	6.7	3.6	48	43	9	10	3.33
B-7	2535.31	46.5	25.7	13.4	10.3	4	44	38	18	10	3.10
B-8	2543.84	54.3	45.7	0	0	0	50	42	8	10	4.04
B-9	2554.03	26	53.1	11.9	6.9	2.2	52	42	6	10	
B-10	2558.28	36.5	32	17.8	8.4	5.3	52	43	5	10	
B-11	2570.89	26.1	45.7	6.2	12.6	8.9	47	51	2	10	4.14
E-1	2076.22	53.6	29.3	8.6	6.3	2.2	48	35	17	5	
E-2	2079.12	50.9	23.7	6.1	15.4	3.9	45	38	17	10	2.7
E-3	2081.43	50.5	26.6	6.8	12	4.1	46	40	14	10	2.83
E-4	2083.32	50	26.6	10.4	9.3	3.7	42	41	17	5	2.78
E-5	2097.00	35.2	34.6	15.1	12.6	2.5	49	42	9	10	
E-6	2098.44	22.1	38.5	17.3	19.2	2.9	48	42	10	10	
E-7	2099.68	32.3	35.6	16.5	12.1	3.5	48	41	11	5	
E-8	2101.86	32.8	36.9	17	11.8	1.5	48	43	9	10	
E-9	2104.44	35.3	34.2	15.9	12.4	2.2	46	43	11	5	
E-10	2107.42	34.9	34.9	15.6	12.3	2.3	49	39	12	10	
E-11	2108.43	35.2	36.4	15.2	10.8	2.4	45	40	15	10	
E-12	2109.31	36.6	37.6	13.2	9.7	2.9	45	42	13	10	
E-13	2113.23	32.5	35.8	18.7	10.2	2.8	47	33	10	10	2.81
E-14	2114.65	26.2	36.8	19.4	15.6	2	49	39	12	10	
E-15	2119.84	35.7	35	14.4	12.2	2.7	49	39	12	5	
E-16	2126.63	33.4	37.2	17.6	9.8	2.1	52	37	11	10	
E-17	2127.53	32.2	39.3	16	10.1	2.4	54	35	11	10	
E-18	2128.47	28.8	41.2	19.6	8.4	2	50	36	14	10	
E-19	2131.68	42.2	31.4	13.2	11.2	2	52	36	12	10	

(continued)

TABLE 1. (*contd.*)

		Mineralogical composition relative percentage (%)					Clay-mineral composition relative percentage (%)				
Sample	Depth (m)	Clay	Quartz	Feldspar	Carbonate	Pyrite	Illite	Mixed-layer	Chlorite	S% in I-S	R_o (%)
E-20	2132.57	37.8	35.2	15.7	9.5	1.8	53	35	12	10	
E-21	2133.92	33.2	40.2	14.5	10.4	1.7	52	40	8	10	
E-22	2138.11	23	39.6	10.6	21.8	5	70	23	7	5	2.76
E-23	2139.75	28.2	37.9	12	15.6	6.3	63	28	9	10	
E-24	2140.45	28.4	40.1	10.6	16.6	4.3	60	30	10	10	
E-25	2141.86	28.3	40.3	11.4	15	5	67	24	9	10	
E-26	2143.63	25.8	43.9	11.2	15.5	3.6	63	31	6	10	
E-27	2144.95	25	45.3	12.3	12.2	5.2	64	29	7	5	
E-28	2147.77	21.6	49.5	7.3	17.7	3.9	60	32	8	10	2.81
E-29	2148.28	22.6	49.5	9.1	18.2	2.9	60	33	7	10	
E-30	2149.58	31.4	44.8	10.4	15.2	2.1	65	26	9	10	2.68
E-31	2150.08	24.3	52.6	9.1	14.5	3	69	27	4	5	
E-32	2150.82	23.2	50.5	9.6	15.1	2.2	62	34	4	5	2.87

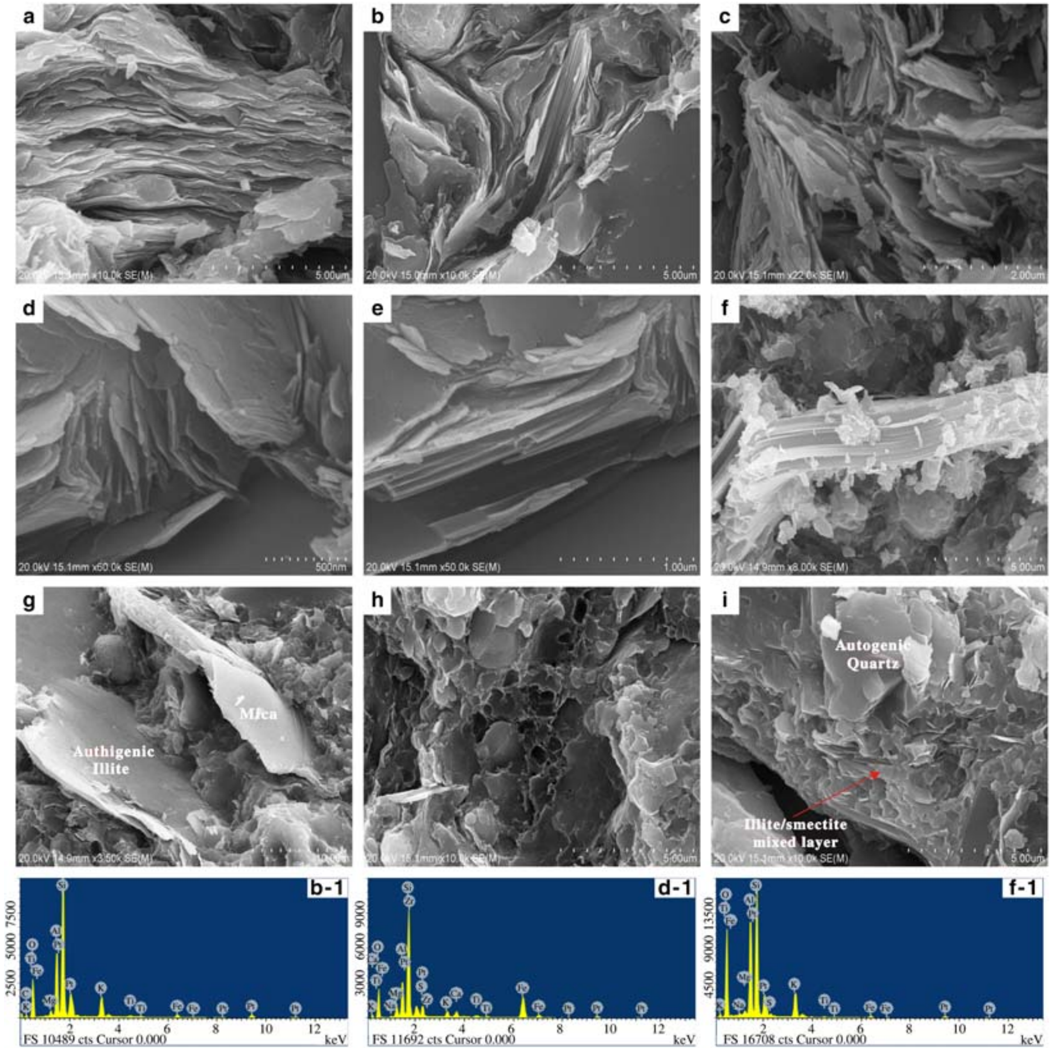

FIG. 2. Microscopic characteristics of clay minerals from the Longmaxi Formation in the East Sichuan Area.

The diagenetic evolution of detrital clays generally follows the reaction sequence of smectite – mixed-layer I-S – kaolinite–illite (Khormali & Abtabi, 2003), and all samples from the study area contain a large amount of mixed-layer I-S. This indicated that smectite illitization is well developed, resulting in a high concentration of diagenetic illite. No samples contain mixed-layer chlorite-smectite minerals, however, indicating that no chloritization of smectite had occurred. In addition, no chlorite of erosional origin was observed in the SEM. Therefore, nearly all chlorite in the clay-mineral assemblages was of detrital origin.

It is generally accepted that the diagenetic illite observed in the SEM would exhibit thread-like or needle-like shapes and would form "bridging" structures between particles (Kang *et al*., 1998). In the present study, however, illite and mixed-layer I-S displayed a strong negative correlation, indicating that the lack of diagenetic illite in SEM images although present, is probably because most clay minerals form coatings on detrital grains in the shale. It is difficult for this illite to form "bridging" structures, therefore. The diagenetic illite is associated with mixed-layer I-S in the form of scales, which are difficult to distinguish in

https://doi.org/10.1180/claymin.2017.052.2.04 Published online by Cambridge University Press

TABLE 2. Chemical composition of clay minerals observed in Fig. 2.

Clay Minerals	MgO (%)	Al_2O_3 (%)	SiO_2 (%)	K_2O (%)	TiO_2 (%)	Fe_2O_3 (%)	(CaO/Na_2O) (%)
Detrital illite (Fig. 2a)	2.59	23.07	63.23	6.33	0.48	3.85	0.44
Detrital illite (Fig. 2b)	2.86	15.58	70.25	6.14		5.17	
Authigenic illite (Fig. 2f)	1.4	30.53	55.3	8.56	0.38	1.78	0.75
Authigenic illite (Fig. 2g)	2.24	30.98	56.22	7.33		2.37	
Mica (Fig. 2g)	2.04	25.33	56.54	9.94	0.41	5.74	
Chlorite (Fig. 2c)	5.48	18.83	65.52	3.55	0.48	5.74	0.4
Chlorite (Fig. 2d)	6.05	21.1	60.59	4.32	0.56	6.72	0.66
Mixed-layer I-S (Fig. 2h)	1.9	14.02	76.56	4.52		3	
Mixed-layer I-S (Fig. 2i)	0.95	12.28	77.44	4.18	0.86	3.29	0.38

the SEM or with EDS analysis. Abundant mixed-layer I-S was observed using the SEM, mostly exhibiting honeycomb-like or scale-like shapes (Fig. 2h,i) and associated with secondary quartz and crystalline pyrite grains (Fig. 2i), These particles had random orientations, and contained intercrystalline pores (Nadeau *et al*., 1985; Peltonen *et al*., 2009).

In summary, the clay minerals in shale from the Longmaxi Formation are mainly detrital and include certain authigenic and diagenetic phases. Detrital clay minerals include mainly illite and chlorite, while authigenic minerals mainly include illite formed by mica weathering, and diagenetic minerals include mainly mixed-layer I-S and illite.

DISCUSSION

Areal distribution and factors controlling occurrences of clay minerals

The clay-minerals content varies between different wells (Fig. 1, Table 3). It increases from the older terranes to the center of the basin, which reflects changes in water depth. Because most chlorite crystals are detrital, the chlorite content in Wells C and D is geographically close to the older terranes in Central Guizhou. Similarly, the chlorite content in Well E exceeds 10% and is geographically close to the Xuefeng Uplift, while that in Well A near the center of the basin is only 6%, indicating a provenance within the eastern Sichuan region from the marginal uplift area.

Illite is derived from terrigenous detritus and is diagenetic in origin. Its content in Well E near the uplift area is greater than that in Wells C and D which are closer to the centre of the basin. This indicates that the illite near the uplift area is mainly detrital, and that its content decreases with increasing distance between the well and the center of the basin. However, the illite content and mixed-layer I-S content increases in Wells A and B, indicating that illite in areas located far from the provenance area mainly derives from smectite illitization rather than terrigenous detritus. The illite content also increases with greater mixed-layer I-S contents, which is the source of the higher illite content in this area, compared to Wells C and D.

In summary, the spatial distribution of clay minerals in the shale of the Longmaxi Formation in the eastern Sichuan Basin is controlled mainly by provenance. The total amount of clay minerals increases while the chlorite content decreases in the direction of source rocks. In areas close to the centre of the basin, the distribution is influenced by diagenesis, and therefore, the illite content first decreases and then increases in the direction of provenance.

TABLE 3. Clay-minerals contents in the various wells at the eastern Sichuan Basin.

Well	Clay-minerals content (wt.%)	Illite (wt.%)	Mixed layer I-S (wt.%)	Chlorite (wt.%)
A	44.9	39.4	54.4	6
B	46.4	47.3	43	11.9
C	38.3	31.8	44.7	23.5
D	40.9	32.3	39.9	27.8
E	34.1	53.8	35.4	10.8

https://doi.org/10.1180/claymin.2017.052.2.04 Published online by Cambridge University Press

Vertical distribution and factors controlling occurrences of clay minerals

The transformation sequence of shale clay minerals in the Longmaxi Formation in eastern Sichuan is: smectite – mixed-layer I-S – illite. The vertical distribution of clay minerals in Well A, shown in Fig. 3, demonstrates that the illite and mixed-layer I-S display a clear trend of decline in one component and increase in another, indicating that formation from a diagenetic process is the main factor controlling illite contents.

In general, the illite content increases and the mixed-layer I-S content decreases with depth, but in the 2380–2410 m section of Well A, the opposite trend is observed. This phenomenon is caused by abnormal high pressure. Hunt (1990) analysed the vertical and horizontal distribution of formation pressures in >180 sedimentary basins around the world, and proposed the existence of an abnormal fluid-pressure "storage box". This type of "storage box", closed in three-dimensions, is isolated from the exterior, forming a separate pressure system. The underlying layers of the stratum between 2380 and 2410 m contain a series of limestone beds with dense lithology, average porosity of 1.58%, average permeability of 1.7×10^{-6} μm^2 and breakthrough pressure of 64.5–70.4 MPa at geothermal temperature of 80°C. The overlying layers contain a series of denser silty shales which represent a shorter interval transit time and greater degrees of compaction. The average porosity is 2.4%, the average permeability is 1.6×10^{-6} μm^2 and the breakthrough pressure is 69.8–701.2 MPa at geothermal temperature of 80°C (Liu, 2015; Zhang *et al*., 2016). Thus, the upper and lower layers have a good sealing effect, this stratum formed a compact closed "storage box" under abnormally high pressure. There are several potential sources of high pressure, which may be produced during structural evolution or in the process of hydrocarbon generation in the source rocks. The pressure coefficient in this layer reaches 1.63–2.18, typical of moderate to ultrahigh pressure (Gao *et al*., 2015). The influence of abnormal high pressures on clay-mineral transformations has been studied extensively in the past: as seen in Fig. 4, for rocks with higher geothermal gradients, the same I content in mixed-layer I-S occurs at shallower depths and at lower temperatures than in rocks with lower geothermal gradients (Perry & Hower, 1970; Hower, 1981). This suggests that greater burial depths must be compensated by higher temperatures. According to Koster van Groos (1987), abnormal high pressure increases the stability of water between smectite layers. Based on Ca-smectite dehydration experiments conducted under simulated burial conditions, Wang & Ouyang (1993) showed that dehydration temperatures rise with increasing water pressures in the absence of foreign components. Buryakovsky *et al.* (1995) proposed that the abnormal pressure gradient is related to the smectite content, where high pressure decreases the smectite dehydration rate, thus increasing the stability of interlayer water. These findings indicate that high pressure inhibits the illitization of smectite. The high pressure is the reason for the abnormal vertical distribution of illite and mixed-layer I-S contents in the lower section of the Longmaxi Formation in Well A.

The Pengshui area, where Well E is located, is closer to the source area of the sediments than the Jiaoshiba area. The chlorite content of the Longmaxi Formation decreases with depth (Fig. 5). This Formation contains a series of siltstone deposits; therefore, the lower member does not necessarily form a "storage box" structure. The occurrence of faults near Well E might be an additional reason for the failure of the "storage box" structure to develop. The acoustic time difference in the lower segment of the Longmaxi Formation also reflects the greater compaction and the absence of abnormal high pressures. Discrete smectite is not present in the Longmaxi Formation, indicating that all smectite has been transformed into interstratified minerals such as mixed-layer I-S. The degree of diagenetic evolution increases with increasing depth. The higher the degree of diagenetic evolution, the greater the amount mixed-layer I-S transformed into illite. Thus, the illite content increases and the abundance of mixed-layer I-S decreases with depth, indicating that diagenesis is the main factor that controls the abundance of illite.

A comparison of Wells A and E shows that with increasing depth, the mixed-layer I-S content increases and the illite content decreases, indicating that smectite illitization is inhibited, probably due to the presence of abnormal high pressure in the enclosed formation. Observation of illite and mixed-layer I-S conversion in closed formations can be used, therefore, as a method for predicting abnormal high pressures.

A pronounced correlation between illite and mixed-layer I-S contents in Well A ($R^2 = 0.95$) indicates that the mixed-layer I-S transforms directly to illite (Fig. 6a). In Well C, the relationship is not as clear ($R^2 = 0.4$) indicating that some of the mixed-layer I-S which is dissolved is not converted to illite (Fig. 6b). Additional K^+ would be necessary during smectite illitization which is compatible with K- feldspar dissolution (Wang *et al*., 2013). The K-feldspar content in the mud shales of the Longmaxi Formation in the study area is much

https://doi.org/10.1180/claymin.2017.052.2.04 Published online by Cambridge University Press

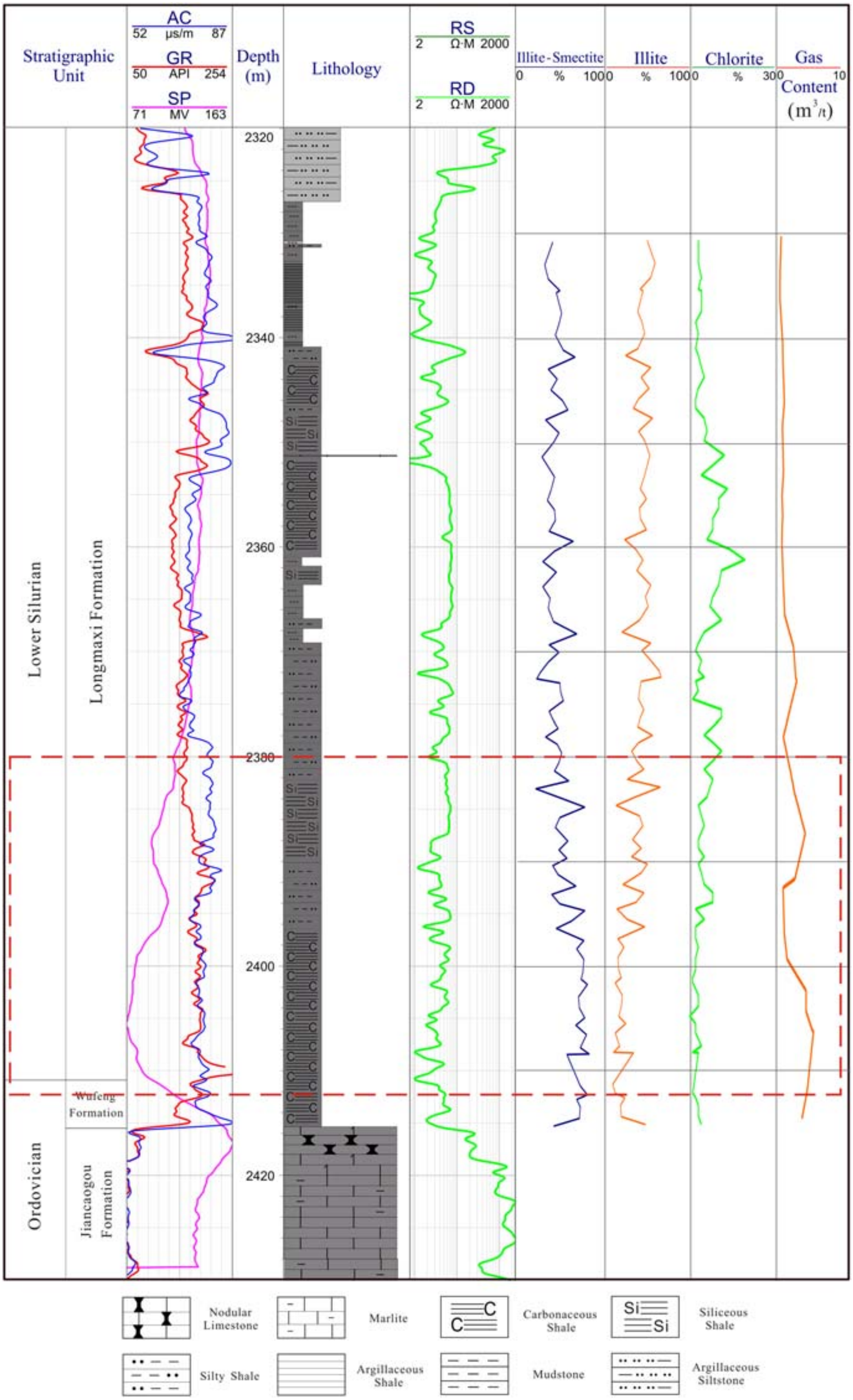

FIG. 3. Lithological section and distribution of clay minerals in Well A.

https://doi.org/10.1180/claymin.2017.052.2.04 Published online by Cambridge University Press

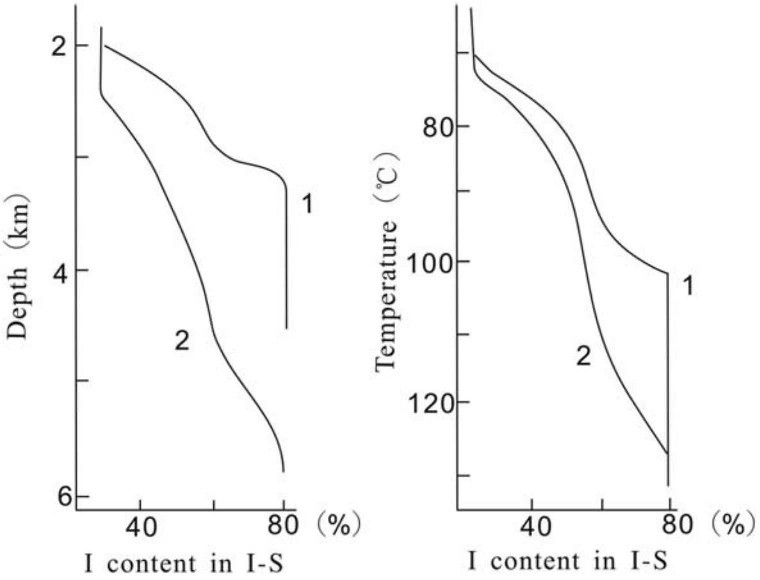

FIG. 4. Relationship between the I content of mixed-layer I-S and the depth and temperature (after Hower, 1981): (1) well with high geothermal gradients (Eocene shale); (2) well with low geothermal gradients (Pliocene-Pleistocene shale).

smaller than that of plagioclase. K-feldspar dissolution is enhanced with increases in depth and temperature, which provides the K^+ required for illitization (Li, J. *et al.*, 2012). Therefore, the above-mentioned phenomena are related to the K-feldspar content. The XRD results show that, although the K-feldspar content in Well A is significantly smaller than that of plagioclase, K-feldspar is present in all samples. In contrast, Well C samples are free of K-feldspar, indicating that the K-feldspar has been dissolved, and that significantly less K^+ would be available for illitization of smectite layers than in Well A. Due to the insufficient K^+ supply, the mixed-layer I-S would not be converted completely to illite.

In summary, the vertical distribution of clay minerals in the Longmaxi Formation in the eastern Sichuan Basin is controlled by the formation mechanism, lithology and degree of compaction. Chlorite is mostly derived from terrigenous detritus and its abundance does not change significantly with depth. The ubiquitous "storage box" structure at the bottom of the Longmaxi Formation resulted in abnormal high pressure, which played a key role in determining the vertical distribution of mixed-layer I-S and illite. Meanwhile, the detrital minerals, especially K-feldspar, also affect the abundances of these phases. The irregular transformation sequence between illite and mixed-layer I-S in a closed formation may reflect the presence of abnormal high pressures in this formation.

Effect of clay minerals on shale pores

Based on extensive previous research (Desbois *et al.*, 2009; Loucks *et al.*, 2009, 2010, 2012; Curtis *et al.*, 2010; Diaz *et al.*, 2010; Passey *et al.*, 2010) and on a large number of SEM images from argon-ion-polished shale samples, the pores were classified according to the scheme of Loucks (2012) and were divided into three categories: interparticle (interP) pores, intraparticle (intraP) pores, and organic matter pores (Fig. 7). Fractures were not addressed in this study because they are poorly developed and their structures are not controlled by a single mineral. Three main types of intraP pores occur in the study area: intraplatelet pores within clay aggregates, intercrystalline pores within pyrite framboids and dissolution pores. Intraplatelet pores are located between mutually supported sheet-like clay minerals, and are distributed parallel to the clay-mineral cleavage planes, often filled with pyrite, apatite or organic matter (Fig. 7b).

The main lithofacies in the study area, from bottom to top, are black siliceous shale, black silty shale and black argillaceous shale (Zhao *et al.*, 2016). These three shale types have different mineralogical compositions, resulting in pore characteristics that vary with the shale lithofacies. The argillaceous shale has a very large clay-mineral content (average ~70%) and contains large amounts of intraplatelet pores in clay

https://doi.org/10.1180/claymin.2017.052.2.04 Published online by Cambridge University Press

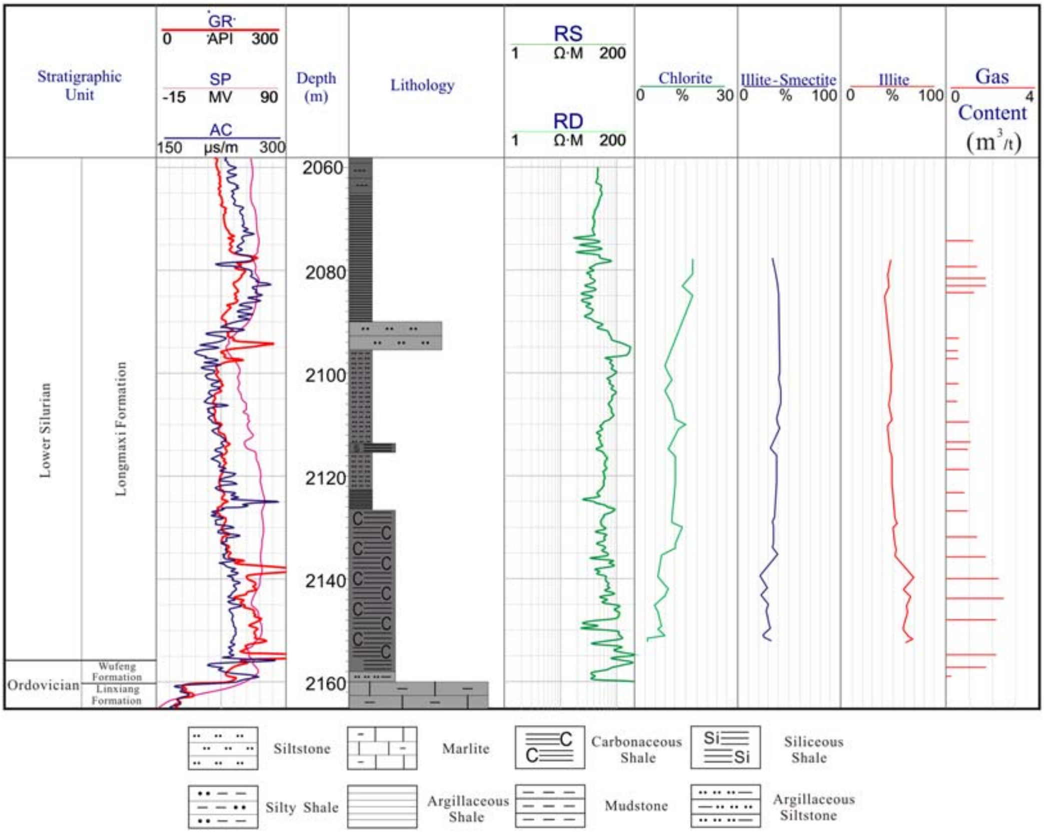

FIG. 5. Lithological column and the distribution of relative clay-minerals contents in Well E.

minerals (Fig. 8a). Brittle mineral particles are dispersed in the shale, most of which are tightly coated by clay minerals (Fig. 8b), with few interP pores. Silty shales have smaller clay-minerals contents (~40% on average), increasing compaction intensity with depth, greater clay mineral density and fewer intraP pores, some of which are preserved by pyrite while others are filled with organic matter (Fig. 8c). In

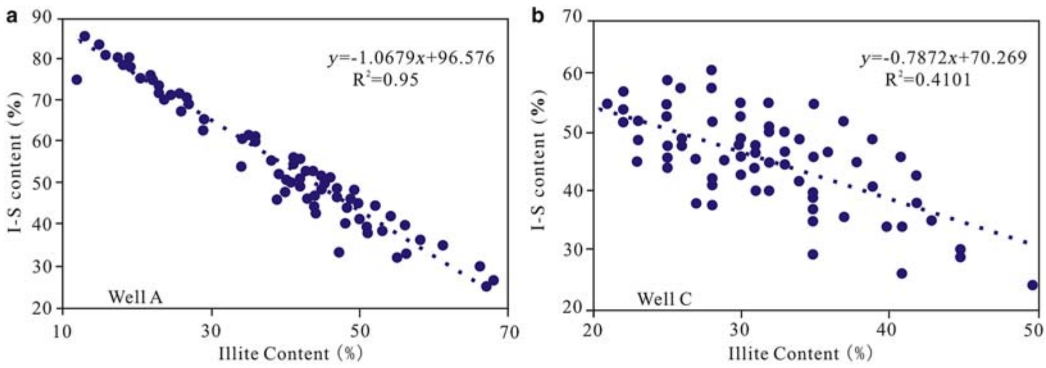

FIG. 6. Relationship between illite (I) content and mixed-layer illite-smectite content (I-S) in the Longmaxi Formation, eastern Sichuan Basin. a = Well A and b = Well C.

https://doi.org/10.1180/claymin.2017.052.2.04 Published online by Cambridge University Press

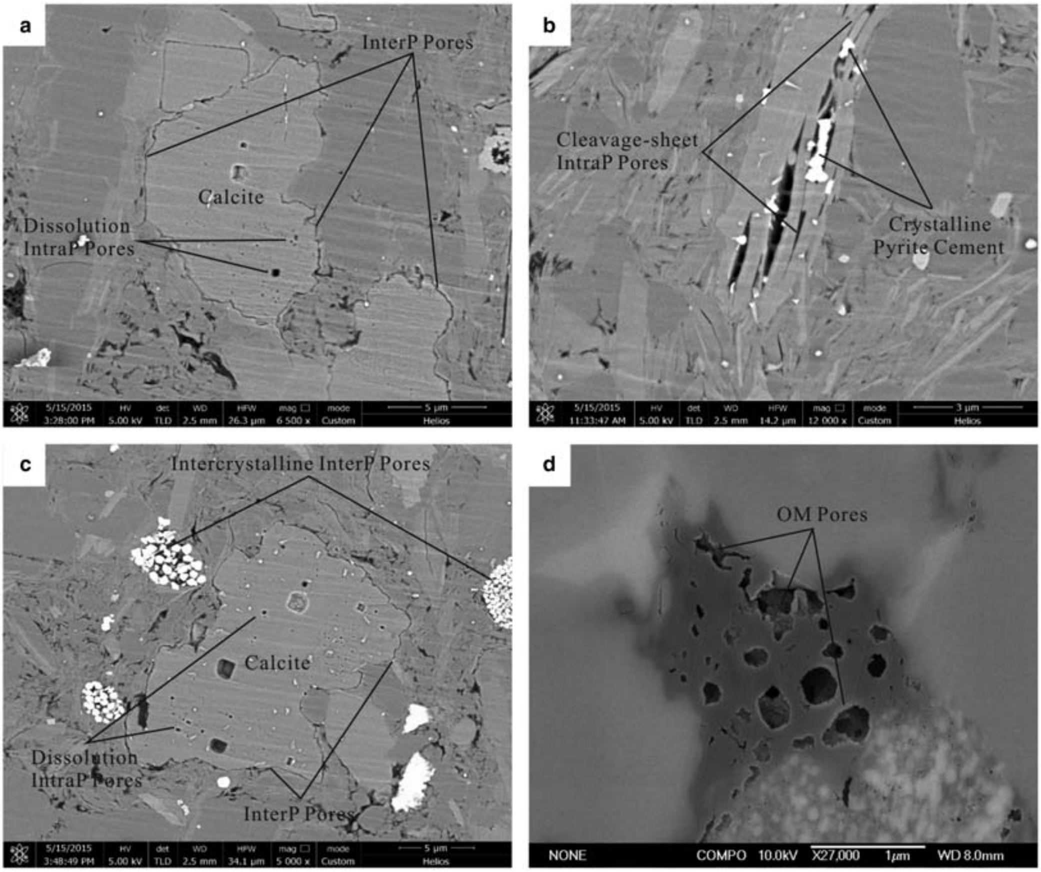

FIG. 7. Characteristics of shale pore types in the Longmaxi Formation in the eastern Sichuan Basin. (a) InterP pores at the edge of calcite particles, black silty shale, Well B, 2495.35 m, S_1ln; (b) Cleavage-sheet intraP pores within clay aggregates, which are partially filled with pyrite, black silty shale, Well B, 2523.11 m, S_1ln; (c) Intercrystalline pores within pyrite framboids and interP pores at the edge of calcite particles, part of which contain dissolution intraP pores, black siliceous shale, Well B, 2558.28 m, S_1ln; (d) slightly directional oval organic matter pores in organic matter, black siliceous shale, Well B, 2565.85 m, S_1ln.

the siliceous shale, up to 60% of the quartz present is authigenic, with a large fraction of silica in the authigenic quartz originating from biogenic silica dissolution and re-precipitation (Zhao *et al*., 2017). The clay minerals make up only ~20% of the rock, and most are filled with organic matter, with rare intraplatelet pores (Fig. 8d).

The clay-minerals contents decrease gradually from top to bottom in the Longmaxi Formation, and the number of intraplatelet pores associated with clay minerals decreases also. Compared with the intercrystalline pores and dissolved pores in pyrite, significant abundances of intraplatelet pores are the main component of intraP pores.

Effect of clay minerals on shale reservoirs

Although the presence of clay minerals is generally a negative factor in evaluations of shale-gas potential (Bowker, 2007), different clay-mineral components have different effects on shale reservoirs for a given constant clay-mineral content. Smectite has a much larger specific surface area than either illite or chlorite, and may contain large quantities of organic matter and adsorbed shale gas (Li & Cai, 2014). Due to the abnormal high pressure in the lower part of the Longmaxi Formation in the Jiaoshiba area, the mixed-layer I-S contains a large amount of adsorbed organic matter, while the “storage box” structure prevented the release of adsorbed organic

https://doi.org/10.1180/claymin.2017.052.2.04 Published online by Cambridge University Press

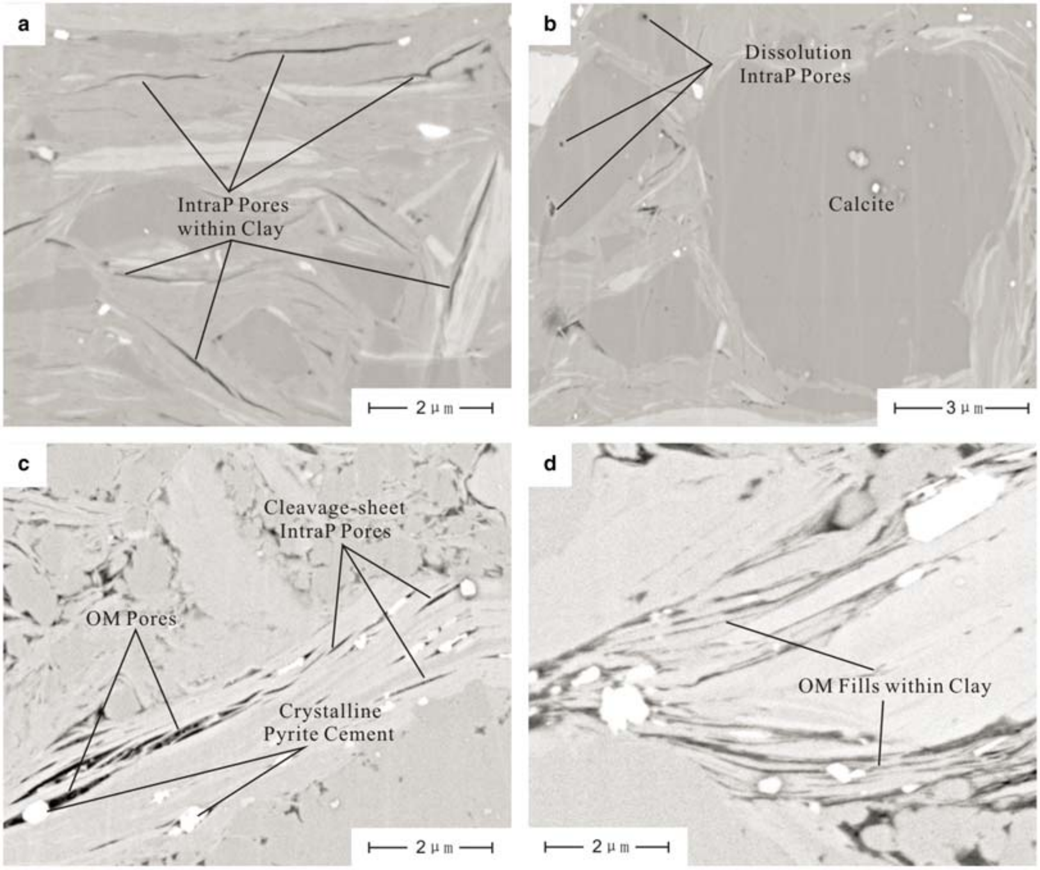

FIG. 8. Pore characteristics in different shale types from the Longmaxi Formation in the eastern Sichuan Basin: (a) intraplatelet pores in clay-mineral particles, black argillaceous shale, Well B, 2,471 m, S_1ln; (b) brittle mineral phases coated densely with clay minerals, without interP pores, but with dissolved pores in some particles, black argillaceous shale, Well B, 2,471 m, S_1ln; (c) clay-mineral particles supported by pyrite-containing cleavage-sheet intraP pores, some of which are filled with organic matter containing organic matter pores, black silty shale, Well B, 2535.31 m, S_1ln; (d) spaces between clay minerals filled with organic matter without intraplatelet pores, black siliceous shale, Well B, 2558.28 m,S_1ln.

matter. This is one reason for the significant increase (>2%) of total organic carbon (TOC) in the lower section of the Longmaxi Formation. Smectite is transformed to mixed-layer I-S releasing interlayer water, which enables a certain amount of intercrystalline pores to form and increases the secondary porosity in shale. At the same time, mixed-layer I-S may adsorb organic matter, which plays a catalytic role in the generation of hydrocarbons from organic matter and leads to the formation of organic pores (Yu *et al*., 2006). Therefore, mixed-layer I-S is more favorable for the formation and preservation of shale gas than illite and chlorite. As a result, smectite and mixed-layer I-S, more than other clay minerals, contribute to the development of shale-gas reservoirs for rocks with a constant clay-mineral content.

CONCLUSIONS

(1) The clay minerals present in the Longmaxi Formation, Eastern Sichuan Basin, China include illite + mixed-layer I-S + chlorite, mainly of clastic origin with some authigenic and diagenetic material. The detrital clay minerals are mainly illite and chlorite, while the authigenic minerals are mainly altered-mica + illite, and the diagenetic minerals are mainly mixed-layer I-S with minor illite.

https://doi.org/10.1180/claymin.2017.052.2.04 Published online by Cambridge University Press

(2) The lithological character of the formation resulted in the formation of a 'storage box' structure in the lower section of the Longmaxi Formation in the Well B of Jiaoshiba area, which was responsible for the development of abnormal high pressure and the inhibition of illitization. An abnormal transformation sequence in which mixed-layer I-S content increased with depth characterizes the vertical clay-mineral distribution. The presence of this abnormal transformation sequence of illite and mixed-layer I-S in closed formations may indicate the presence of abnormal high pressures in the formation. The detrital composition affected the mixed-layer I-S and illite contents indirectly, particularly in terms of the K-feldspar abundance. The availability of sufficient K^+ during the conversion of mixed-layer I-S to illite determined the extent of transformation.

(3) Interparticle pores, intraparticle pores and organic matter pores were observed in the shale reservoir rocks of the Longmaxi Formation. Among these, the intraparticle pores can be subdivided into intraplatelet pores within clay aggregates, intercrystalline pores within pyrite framboids and dissolution pores. The clay-mineral contents control the degree of intraparticle pore development, which are mainly composed of intraplatelet pores.

(4) Compared with other clay minerals, smectite and mixed-layer I-S contribute more to the development of shale-gas reservoirs given a constant clay-mineral content. The lower section of the Longmaxi Formation of Jiaoshiba area experienced abnormal high pressure, resulting in an increase in the mixed-layer I-S content. The transformation of smectite into mixed-layer I-S released interlayer water, resulting in the formation of intercrystalline pores, which increased the secondary porosity in the shale. In addition, organic matter and shale gas might have been adsorbed to mixed-layer I-S particles. This has a positive effect on the formation and storage of shale gas and provides more favorable conditions for the development of shale-gas reservoirs.

ACKNOWLEDGEMENTS

This research was supported by the China Postdoctoral Science Foundation (No. 2016M591350).

REFERENCES

Anderson J.L. & Rowley M.C. (1981) Synkinematic intrusion of peraluminous and associated metaluminous granitic magmas, Whipple Mountains, California. *The Canadian Mineralogist*, **19**, 83–101.

Bowker K.A. (2007) Barnett shale gas production, Fort Worth Basin: Issues and discussion. *AAPG Bulletin*, **91**, 523–533.

Buryakovsky L.A., Rashid D.D. & Chilingar G.V. (1995) Abnormally high formation pressure in Azerbaijan and the South Caspian Basin. *Journal of Petroleum Science and Engineering*, **13**, 203–218.

Curtis M.E., Ambrose R.J., Sondergeld C.H. & Rai C.S. (2010) Structural characterization of gas shales on the micro- and nano-scales. SPE Paper 137693 in: *Canadian Unconventional Resources and International Petroleum Conference*, Calgary, Alberta, Canada.

Daoudi L., Ouajhin B. & Rocha F. (2010) Comparative influence of burial depth on the mineral assemblage of the Agadir-Essaouira Basin (western High Atlas, Morocco). *Clay Minerals*, **45**, 453–467.

Desbois G., Urai J.L. & Kukla P.A. (2009) Morphology of the pore space in claystones – Evidence from BIB/FIB ion beam sectioning and cryo-SEM observations. *Earth*, **4**, 15–22.

Diaz E., Sisk C. & Nur A. (2010) Quantifying and linking shale properties at a variable scale. ARMA Paper 10-272. In: *44th U.S. Rock Mechanics Symposium and 5th U.S.-Canada Rock Mechanics Symposium*, Salt Lake City, Utah, USA.

Fu X., Qin J. & Teng G. (2011) Mineral components of source rocks and their petroleum significance: A case from Paleozoic marine source rocks in the Middle–Upper Yangtze region. *Petroleum Exploration and Development*, **38**, 671–684.

Gao J., He S. & Yi J. (2015) Discovery of high density methane inclusions in Jiaoshiba shale gas field and its significance. *Oil and Gas Geology*, **36**, 472–480.

Guo Y., Li Z. & Li D. (2004) Lithofacies palaeogeography of the Early Silurian in the Sichuan area. *Journal of Palaeogeography*, **6**, 20–29.

Hillier S. (1995) *Sedimentation and Sedimentary Origin of Clays*. Springer-Verlag, Berlin, pp. 162–219.

Hower J. (1981) Shale diageneses. Pp. 66–70 in: *Clays and the Resource Geologist* (F.J. Longstrafte, editor). Short Course Handbook **7**, Mineralogical Association of Canada.

Hunt J.M. (1990) Generation and migration of petroleum from abnormal pressure fluid compartments. *AAPG Bulletin*, **74**, 1–12.

Jin N., Li A. & Liu H. (2007) Clay minerals in surface sediment of the northwest Parece Vela Basin: distribution and provenance. *Oceanologia et Limnologia Sinica*, **38**, 504–511.

Jin Y., Cai X., Yuan Y. & Wu Y. (2015) Clay mineral characteristics and geological significance in Silurian Longmaxi Formation Shale, southeastern Chongqing. *Coal Geology of China*, **27**, 21–25.

Kang Y., Luo P. & Jiao K. (1998) Clay minerals and potential formation damage of tight gas bearing sandstone in West Sichuan. *Journal of Southwest Petroleum University*, **20**, 1–5.

Khormali F. & Abtabi A. (2003) Origin and distribution of clay minerals in calcareous arid and semi-arid soils of Fars Province, southern Iran. *Clay Minerals*, **38**, 511–527.

Koster van Groos A.F. & Guggenheim S. (1987) High-pressure differential thermal analysis (HP -DTA) of the dehydroxylation of Na-rich montmorillonite and K-exchanged montmorillonite. *American Mineralogist*, **72**, 1170–1175.

Li J., Yu B. & Liu C. (2012) Clay minerals of black shale and their effect on physical properties of shale gas reservoirs in the southeast of Chongqing: A case study from Lujiao outcrop section in Pengshui, Chongqing. *Geoscience*, **26**, 732–740.

Li Y. & Cai J. (2014) Effect of smectite illitization on shale gas occurrence in argillaceous source rocks. *Petroleum Geology and Experiment*, **36**, 352–358.

Li Y., Fan T. & Gao Z. (2012) Sequence stratigraphy of Silurian Black Shale and its distribution in the southeast area of Chongqing. *Natural Gas Geoscience*, **23**, 299–306.

Liang S., Gan F., Yan B. & Wang R. (2012) Relationship between composition and spectral feature of muscovite. *Remote Sensing for Land & Resources*, **24**, 111–115.

Liu R. (2015) Analyses of influences on shale reservoirs of Wufeng-Longmaxi Formation by overpressure in the Southeastern part of Sichuan Basin. *Acta Sedimentologica Sinica*, **33**, 817–827.

Liu S.G., Wang S.Y., Sun W., Ran B. & Yang D. (2013) Characteristics of black shale in Wufeng Formation and Longmaxi Formation in Sichuan Basin and its peripheral areas. *Journal of Chengdu University of Technology*, **40**, 621–639.

Liu Y., Di S. & Xue X. (1998) Clay minerals from the Lower Cretaccous to Middle Jurassic strata in the Bazhou depression, eastern Qilian folded belt. *Journal of Palaeogeography*, **18**, 10–15.

Liu Y., Yu B. & Zhu J. (2009) Diagenesis of Paleogene clastic reservoir in Liaohe River and its influence on reservoir properties. *Modern Geology*, **23**, 731–738.

Loucks, R.G., Reed R.M., Ruppel S.C. & Jarvie D.M. (2009) Morphology, genesis, and distribution of nanometer-scale pores in siliceous mudstones of the Mississippian Barnett Shale. *Journal of Sedimentary Research*, **79**, 848–861.

Loucks, R.G., Reed R.M., Ruppel S.C. & Hommes U. (2010) Preliminary classification of matrix pores in mudrocks. *Gulf Coast Association of Geological Societies Transactions*, **60**, 435–441.

Loucks R.G., Reed R.M., Ruppel S.C. & Hommes U. (2012) Spectrum of pore types and networks in mudrocks and a descriptive classification for matrix-related mudrock pores. *AAPG Bulletin*, **96**, 1071–1098.

Ma L., Chen H. & Gan K. (2004) *Tectonic and Marine Petroleum Geology in the South of China*. Geological Publishing House, Beijing, pp. 52–98.

Miller C.F., Stoddard E.F., Bradfish L.J. & Dollase W.A. (1981) Composition of plutonic muscovite: Genetic implications. *The Canadian Mineralogist*, **19**, 25–34.

Nadeau P.H., Wilson M.J., McHardy W.J. & Tait J.M. (1985) The conversion of smectite to illite during diagenesis: Evidence from some illitic clays from bentonites and sandstones, diagenesis and low-temperature metamorphism. *Mineralogical Magazine*, **49**, 393–400.

Passey Q.R., Bohacs K.M., Esch W.L., Klimentidis R. & Sinha S. (2010) *From oil-prone source rock to gas-producing shale reservoir: Geologic and petrophysical characterization of unconventional shale-gas reservoirs*. SPE Paper 131350 in: *International Oil and Gas Conference and Exhibition*, Beijing, China.

Peltonen C., Marcussen Ø. & Bjørlykke K. (2009) Clay mineral diagenesis and quartz cementation in mudstones: the effects of smectite to illite reaction on rock properties. *Marine and Petroleum Geology*, **26**, 887–898.

Perry E.A. & Hower J. (1970) Burial diagenesis in Gulf coast politic sediments. *Clays and Clay Minerals*, **28**, 165–177.

Strixrude L. & Peacor D.R. (2002) First-principles study of illite–smectite and implications for clay mineral systems. *Nature (London)*, **420**, 165–168.

Su W.B., He L.Q., Wang Y.B., Gong S.Y. & Zhou H.Y. (2002) The bentonite and high resolution composite formation at the bottom of Wufeng-Longmaxi Formation (Ordovician-Silurian), South China. *Science in China (Series D)*, **32**, 207–219.

Sun Y., Yang F. & Luo J. (1998) Application of clay minerals in petroleum exploration in Tarim Basin. *Modern Geology*, **12**, 269–276.

Wang S. & Ouyang Z. (1993) Study on influence of pressure in the dehydration of calcium smectite. *Science Bulletin*, **28**, 243–246.

Wang K., Orth C.J. & Attrep M. (1993) The great latest Ordovician extinction on the South China Plate: chemostratigraphic studies of the Ordovician-Silurian boundary interval on the Yangtze Platform Event markers in Earth history. *Palaeogergraphy, Palaeoclimatology, Palaeoecology*, **104**, 61–79.

Wang X., Mou C. & Gong Y. (2013) Diagenetic evolution and facies of the reservoir in section 8 of Permian Shihezi Formation He8 section of Z30 block of the Sulige Gas Field. *Acta Petrolei Sinica*, **34**, 883–895.

Wang X., Mou C. & Ge X. (2014) Study on clay minerals in the lower Silurian Longmaxi Formation in southern Sichuan Basin and its periphery. *Natural Gas Geoscience*, **25**, 1781–1794.

Wu X., Liu C. & Ju J. (1997) The identification method of neoformed, inherited and transformed clay minerals. *Journal of Xianning Normal College: Science and Technology Edition*, **17**, 74–76.

Yu H., Xie J. & Wang X. (2006) Organoclay complexes in relation to petroleum generation. *Earth Science Frontiers*, **13**, 274–281.

Zeng X., Liu S. & Huang W. (2011) Comparison of Silurian Longmaxi Formation shale of Sichuan Basin in China and Carboniferous Barnett Formation shale of Fort Worth Basin in United States. *Geological Bulletin of China*, **30**, 372–384.

Zhang B., Wu J., Ling H. & Chen P. (2010) Petrological discrimination between primary and secondary muscovites and its geological implications: A case study of Fucheng peraluminous granite pluton in southern Jiangxi. *Acta Petrologica et Mineralogica*, **29**, 225–234.

Zhang H., Wang Q., Ni K. & Li C. (2016) Six characteristics and main controlling factors of shale reservoirs in the Wufeng-Longmaxi formations, southeastern Sichuan Basin. *Petroleum Geology & Experiment*, **38**, 320–332.

Zhang Z., Hu P. & Shen J. (2013) Mineral compositions and organic matter occurrence modes of Lower Silurian Longmaxi Formation of Sichuan Basin. *Journal of China Coal Society*, **38**, 766–771.

Zhang R. (1992) Application of scanning electron microscopy to study of mineral change – transformation of feldspar into clay minerals. *Scientia Geological Sinica*, **1**, 66–70.

Zhao J., Jin Z., Jin Z., Wen X., Geng Y., Yan C. & Nie H. (2016) Lithofacies and sedimentary environment of shale in Wufeng–Longmaxi Formation, Sichuan Basin. *Acta Petrolei Sinica*, **37**, 572–586.

Zhao J., Jin Z., Jin Z., Wen X. & Geng Y. (2017) Origin of authigenic quartz in organic-rich shales of the Wufeng and Longmaxi Formations in the Sichuan Basin, South China: Implications for pore evolution. *Journal of Natural Gas Science and Engineering*, **38**, 21–38.

Zhao X. & He D. (2008) Clay mineral analysis and some problems of application in petroleum geology. *Xinjiang Petroleum Geology*, **29**, 756–758.

Zhou C., Luo R. & Li Z. (2005) The application of scanning electron microscopy in the study of clay minerals in clastic reservoir. *Natural Gas Exploration and Development*, **28**, 4–8.

https://doi.org/10.1180/claymin.2017.052.2.04 Published online by Cambridge University Press